



Alexandria University
Alexandria Engineering Journal

www.elsevier.com/locate/aej
www.sciencedirect.com



ORIGINAL ARTICLE

Steady state response of functionally graded nano-beams resting on viscous foundation to super-harmonic excitation



Sima Ziaee

Department of Mechanical Engineering, Yasouj University, Yasouj, Iran

Received 6 February 2015; revised 9 April 2016; accepted 25 June 2016

Available online 20 July 2016

KEYWORDS

FG nano-beams;
 Nonlinear forced vibration;
 Viscous foundation;
 Super-harmonic excitation;
 Nonlocal elasticity

Abstract This article attempts to investigate the effects of small scale parameter on steady state response of functionally graded nano-beams resting on a viscous foundation to super-harmonic excitation. A simple power-law distribution is used to model the variation of material property graded in the thickness direction. The dimensionless partial differential equation of motion is derived by using Euler-Bernoulli beam theory, von-Karman geometric nonlinearity and Eringen's nonlocal elasticity theory. Using multiple scale method, one can find the governing equations of steady state response of functionally graded nano-beams excited by distributed harmonic force. The small scale parameter (e_0a) is changed between 0 and 2 to investigate the effects of small scale on steady state response of excited functionally graded nano-beams due to lack of information. The study of the effects of small scale parameter on backbone curves shows that an increase in the small scale parameter often decreases the dimensionless peak response although the type of loading can change the relationship between small scale parameter and the dimensionless peak response.

© 2016 Faculty of Engineering, Alexandria University. Production and hosting by Elsevier B.V. This is an open access article under the CC BY-NC-ND license (<http://creativecommons.org/licenses/by-nc-nd/4.0/>).

1. Introduction

Functionally graded materials (FGM) have unique characteristics resulting from the smooth and continuous variation of properties along certain dimensions. These remarkable advantages have made them the notable materials which can be used in many engineering application fields [1]. The growing development of technology has permitted the use of FGM thin beams in micro/nano-electro-mechanical systems, such as

electrically actuated devices and atomic force microscopes [2], so the study of mechanical behavior of FG micro-/nano-beams has recently become a topic of interest to researchers.

Using a modified couple stress theory, Reddy [3] derived the nonlinear non-classical Timoshenko and Euler-Bernoulli beam theories to study static bending, free vibration, and buckling of FG simply supported micro-beams. These theories were used by Arbind and Reddy [4] to investigate nonlinear bending response of clamped FG micro-beams under mechanical loadings while Eltaher et al. [5,6] and Şimşek and Yurtcu [7] independently employed nonlocal Timoshenko beam theory [5,7] and nonlocal Euler-Bernoulli beam theory [6,7] to study the static bending and buckling of FG nano-beams with different boundary conditions. Some researchers used the

E-mail addresses: simaziae@gmail.com, sima_ziaee@yahoo.com, Ziaee@yu.ac.ir

Peer review under responsibility of Faculty of Engineering, Alexandria University.

<http://dx.doi.org/10.1016/j.aej.2016.06.028>

1110-0168 © 2016 Faculty of Engineering, Alexandria University. Production and hosting by Elsevier B.V.

This is an open access article under the CC BY-NC-ND license (<http://creativecommons.org/licenses/by-nc-nd/4.0/>).

combination of surface elasticity theory [8,9] or the strain gradient theories [10–12] with nonlinear beam theories to study nonlinear free vibration of functionally graded nano-beams as well.

All analytical and numerical results reported by researchers mentioned above clearly show the difference between classical and non-classical continuum theories in predicting mechanical behavior of size-dependent FG beams. Due to the necessity of incorporating the size effect into classical continuum mechanics to study mechanical behavior of FG micro-/nano-beams accurately, the nonlocal elasticity theory has been employed to simulate dynamical behavior of micro/nano-beams by some researchers.

Eltaher et al. [13] studied free vibration of FG nano-beams based upon nonlocal Euler-Bernoulli beam theory and finite element method. The effects of neutral axis location on linear natural frequencies of FG macro-/nano-beams were investigated by Eltaher et al. [14] as well. Uymaz [15] used generalized beam theory and the nonlocal elasticity to present forced vibration of FG nano-beams. Nonlinear free vibration of FG nano-beams was studied by Nazemnezhad and Hosseini-Hashemi [16] based on nonlocal Euler-Bernoulli beam theory and multiple scale method. Using nonlocal Timoshenko beam theory, Rahmani and Pedram [17] investigated the effects of gradient index and geometrical dimensions on linear free vibration of FG nano-beams. He's variational method and nonlocal Euler-Bernoulli beam theory were used to study the large amplitude free vibration of FG nano-beams resting on nonlinear elastic foundation by Niknam and Aghdam [18]. Kiani [19] proposed a mathematical model to investigate the vibration and instability of moving FG nano-beams based on nonlocal Rayleigh beam theory. Obtained results clearly show that the value of small scale parameter is an important factor to estimate dynamic responses of FG nano-beams accurately although boundary conditions, order of the mode of vibration and geometrical dimensions can affect the role of the small scale parameter in simulating dynamic responses of FG nano-beams.

Although it is well known that proper values of the nonlocal parameter must be used if the accurate study of mechanical behavior of micro-/nano-structures is desired, a thorough research has not been done to estimate the value of small scale corresponding to mechanical response of functionally graded micro-/nano-beams so far [16]. Hence, all researchers who used nonlocal continuum theories to simulate size-dependent mechanical behavior of FG nano-beams investigated the effects of small scale parameter on mechanical behavior of FG nano-beams by changing the value of the small scale parameter [13–16].

Based upon the author's knowledge, there is no notable study showing the influence of nonlocal parameter on mechanical response of FG nano-beams to sub- or super-harmonic excitation. So, the investigation of the effects of small scale parameter on steady-state response of FG nano-beams resting on a viscous foundation to super-harmonic excitation is the main purpose of this article. A simple power-law distribution is used to model the variation of material property graded in the thickness direction. The partial differential equation of motion is derived based on Euler-Bernoulli beam theory, von-Karman geometric nonlinearity and Eringen's nonlocal elasticity theory. The multiple scale method is employed to find

governing equations of steady state response of FG nano-beams excited by distributed harmonic force. In the parametric studies of this work, due to lack of information, small scale (e_0a) is varied between 0 and 2 to investigate the effects of small scale on steady state response of excited FG nano-beams.

2. Equation of motion

The following equation is the partial differential equation of motion of a simply supported FG nano-beam resting on viscous foundation (Fig. 1) with length L , width b and thickness h and immovable ends. This equation is derived based on Euler-Bernoulli beam theory hypothesis, von-Karman geometric nonlinearity and Eringen's nonlocal elasticity theory (details can be found in Appendix A):

$$(e_0a)^2 H + \hat{N} \frac{\partial^2 W}{\partial x^2} - \hat{k} W - \hat{c} \frac{\partial W}{\partial t} + F(x, t) = \left(\int_{A_0} (z - z_0)^2 E(z) dA_0 \right) \frac{\partial^4 W}{\partial x^4} + \left(\int_{A_0} \rho(z) dA_0 \right) \frac{\partial^2 W}{\partial t^2} \quad (1)$$

where H is defined by Eq. (2):

$$H = \hat{c} \frac{\partial^3 W}{\partial x^2 \partial t} + \hat{k} \frac{\partial^2 W}{\partial x^2} - \frac{\partial^2 F}{\partial x^2} - \hat{N} \frac{\partial^4 W}{\partial x^4} + \left(\int_{A_0} \rho(z) dA_0 \right) \frac{\partial^4 W}{\partial x^2 \partial t^2} \quad (2)$$

and \hat{N} is as follows:

$$\hat{N} = + \frac{1}{2L} \left(\int_{A_0} E(z) dA_0 \right) \int_0^L \left(\frac{\partial W}{\partial x} \right)^2 dx \quad (3)$$

where $W = W(x, t)$ denotes the transverse displacement of any point on the geometric mid-plane ($z = 0$, based on Fig. 1) of beam element, $\rho(z)$ is mass density which is functionally graded in the thickness direction, \hat{k} and \hat{c} are the stiffness of the foundation and the damping coefficient of the foundation respectively, $F = F(x) \cos(\Omega t)$ is a transverse loading, and e_0a is a material length scale parameter which contains material constant and internal characteristic length. The distance of the neutral surface of the FG nano-beam from the geometric mid-plane of the FG nano-beam ($z = 0$, based on Fig. 1) is shown by z_0 [14].

One can employ the following dimensionless variables to simplify the parametric studies [20]:

$$\bar{x} = \frac{x}{L}, \quad \bar{W} = \frac{W}{r}, \quad \bar{t} = t \sqrt{D/\rho_e L^4},$$

$$D = b \int_{-\frac{h}{2}}^{\frac{h}{2}} z^2 E(z) dz, \quad \rho_e = b \int_{-\frac{h}{2}}^{\frac{h}{2}} \rho(z) dz, \quad A = b \int_{-\frac{h}{2}}^{\frac{h}{2}} E(z) dz, \quad (4)$$

$$r = \sqrt{bh^3/12(bh)}$$

Then, the governing partial differential equation of motion changes to the following:

$$\frac{-L^4 (e_0a)^2}{rD} \bar{H} + \frac{\partial^2 \bar{W}}{\partial \bar{t}^2} + \frac{\partial^4 \bar{W}}{\partial \bar{x}^4} + \frac{\hat{k} L^4}{D} \bar{W} + \frac{\hat{c} L^2}{\sqrt{D\rho_e}} \frac{\partial \bar{W}}{\partial \bar{t}} - \left(\frac{Ar^2}{2D} \int_0^1 \left(\frac{\partial \bar{W}}{\partial \bar{x}} \right)^2 d\bar{x} \right) \frac{\partial^2 \bar{W}}{\partial \bar{x}^2} = F \frac{L^4}{rD} \quad (5a)$$

where

$$\bar{H} = -\frac{1}{L^2} \frac{\partial^2 F}{\partial \bar{x}^2} + \frac{\hat{k}r}{L^2} \frac{\partial^2 \bar{W}}{\partial \bar{x}^2} + \frac{\hat{c}r}{L^2} \sqrt{\frac{D}{\rho_e L^4}} - \left[\frac{Ar^3}{2L^6} \int_0^1 \left(\frac{\partial \bar{W}}{\partial \bar{x}} \right)^2 d\bar{x} \right] \frac{\partial^4 \bar{W}}{\partial \bar{x}^4} + [Dr/L^6] \frac{\partial^4 \bar{W}}{\partial \bar{x}^2 \partial \bar{t}^2} \quad (5b)$$

If the small scale parameter (e_0a) and the index of power-law (\bar{n}) in Eq. (5) are taken equal to zero, Eq. (5) will be converted to the well-known local equation of nonlinear lateral vibration of homogeneous beams obtained and used in some papers [21].

To estimate transverse displacement of simply supported FG nano-beams, one can use the mode shapes of linear vibration of nano-beams:

$$\bar{W} = \sum_{s=1}^N \bar{q}_s(\bar{t}) \sin(s\pi\bar{x}) \quad (6)$$

The partial differential equation changes to the system of ordinary differential equations by substituting Eq. (6) for \bar{W} in Eq. (5) and using Galerkin method:

$$\ddot{\bar{q}}_s + (\bar{\omega}_s)^2 \bar{q}_s + \bar{C}_s \dot{\bar{q}}_s = -a_s \bar{q}_s \sum_{m=1}^N m^2 (\bar{q}_m)^2 + (\hat{F}_s - (e_0a)^2 \hat{G}_s) \cos(\bar{\Omega}\bar{t}) \quad (7)$$

where

$$(\bar{\omega}_s)^2 = \frac{\hat{k}L^4}{D} + \frac{(s\pi)^4}{\frac{(e_0a)^2 (s\pi)^2}{L^2} + 1} \quad (8)$$

$$a_s = \frac{Ar^2}{4D} s^2 \pi^4 \quad (9a)$$

$$\bar{C}_s = \frac{\hat{c}L^2}{\sqrt{D\rho_e}} \quad (9b)$$

$$\hat{F}_s - (e_0a)^2 \hat{G}_s = \frac{2}{\frac{(e_0a)^2 (s\pi)^2}{L^2} + 1} \int_0^1 \left(F(\bar{x}) \frac{L^4}{rD} - \frac{(e_0a)^2 L^2}{rD} \frac{\partial^2 F(\bar{x})}{\partial \bar{x}^2} \right) \sin(s\pi\bar{x}) d\bar{x} \quad (9c)$$

and s is half-wavelength number. $\bar{\omega}_s$ is also s th dimensionless linear natural frequency of FG nano-beams obtained by omitting the nonlinear terms and external load from Eq. (7).

3. Super-harmonic excitation

According to the multiple scale method, the solution of the system of ordinary differential equations (7) is approximated as follows:

$$\bar{q}_s = \varepsilon \bar{q}_{s1}(T_0, T_2) + \varepsilon^3 \bar{q}_{s3}(T_0, T_2) \quad (10)$$

where $T_2 = \varepsilon^2 \bar{t}$, $T_0 = \bar{t}$ and ε is a small dimensionless parameter. The slow scale $T_1 = \varepsilon \bar{t}$ and the term $\varepsilon^2 \bar{q}_{s2}$ are omitted from Eq. (10) because the nonlinearity is cubic [22]. To show the damping terms and the nonlinear terms in the same perturbation equations, one must set the damping coefficients (\bar{C}_s) to $2\varepsilon^2 \bar{C}_s$. It is not necessary to scale the forcing terms because the excitation terms must be appeared in equations resulting from equating the coefficient of ε^1 . The following equations are obtained by substituting Eq. (10) for \bar{q}_s into Eq. (7) and equating coefficients of like powers of ε :

$$D_0^2 \bar{q}_{s1} + (\bar{\omega}_s)^2 \bar{q}_{s1} = (\hat{F}_s - (e_0a)^2 \hat{G}_s) \cos(\bar{\Omega}\bar{t}) \quad (11)$$

$$D_0^2 \bar{q}_{s3} + 2D_0 D_2 \bar{q}_{s1} + (\bar{\omega}_s)^2 \bar{q}_{s3} + 2\hat{C}_s D_0 \bar{q}_{s1} = -a_s \bar{q}_{s1} \sum_{m=1}^N m^2 q_{m1}^2 \quad (12)$$

where $D_n = \frac{\partial}{\partial T_n}$. One can write the solution of Eq. (11) as follows:

$$\bar{q}_{s1} = A_s(T_2) \exp(i\bar{\omega}_s T_0) + \frac{(\hat{F}_s - (e_0a)^2 \hat{G}_s)}{2(\bar{\omega}_s^2 - \bar{\Omega}^2)} \exp(i\bar{\Omega} T_0) + CC \quad (13)$$

where CC stands for complex conjugate of the preceding terms.

Substituting Eq. (13) for \bar{q}_{s1} into Eq. (12) yields the following:

$$D_0^2 \bar{q}_{s3} + (\bar{\omega}_s)^2 \bar{q}_{s3} = - \left(i\bar{\omega}_s 2\hat{C}_s A_s \exp(i\bar{\omega}_s T_0) + i\hat{C}_s \bar{\Omega} \frac{(\hat{F}_s - (e_0a)^2 \hat{G}_s)}{2(\bar{\omega}_s^2 - \bar{\Omega}^2)} \exp(i\bar{\Omega} T_0) \right) - \left(i2\bar{\omega}_s \frac{dA_s}{dT_2} \exp(i\bar{\omega}_s T_0) \right) - a_s \sum_{m=1}^N m^2 (q_{s1} q_{m1}^2) + CC \quad (14)$$

where

$$\begin{aligned} \bar{q}_{s1} \bar{q}_{m1}^2 = & \frac{A_s A_m (\hat{F}_m - (e_0a)^2 \hat{G}_m)}{(\bar{\omega}_m^2 - \bar{\Omega}^2)} \exp(iT_0(\bar{\omega}_m + \bar{\omega}_s + \bar{\Omega})) \\ & + A_m^2 A_s \exp(iT_0(2\bar{\omega}_m + \bar{\omega}_s)) + 2A_m \bar{A}_m A_s \exp(i\bar{\omega}_s T_0) \\ & \frac{A_s (\hat{F}_m - (e_0a)^2 \hat{G}_m)^2}{4(\bar{\omega}_m^2 - \bar{\Omega}^2)^2} \exp(iT_0(\bar{\omega}_s + 2\bar{\Omega})) \\ & + \frac{A_s (\hat{F}_m - (e_0a)^2 \hat{G}_m)^2}{2(\bar{\omega}_m^2 - \bar{\Omega}^2)^2} \exp(iT_0 \bar{\omega}_s) \\ & + A_m^2 \bar{A}_s \exp(iT_0(2\bar{\omega}_m - \bar{\omega}_s)) \\ & + \frac{A_s A_m (\hat{F}_m - (e_0a)^2 \hat{G}_m)}{(\bar{\omega}_m^2 - \bar{\Omega}^2)} \exp(iT_0(\bar{\omega}_m + \bar{\omega}_s - \bar{\Omega})) \\ & + \frac{A_s (\hat{F}_m - (e_0a)^2 \hat{G}_m)^2}{4(\bar{\omega}_m^2 - \bar{\Omega}^2)^2} \exp(iT_0(\bar{\omega}_s - 2\bar{\Omega})) \\ & + \frac{A_s \bar{A}_m (\hat{F}_m - (e_0a)^2 \hat{G}_m)}{(\bar{\omega}_m^2 - \bar{\Omega}^2)} \exp(iT_0(\bar{\omega}_s - \bar{\omega}_m - \bar{\Omega})) \\ & + \frac{A_s \bar{A}_m (\hat{F}_m - (e_0a)^2 \hat{G}_m)}{(\bar{\omega}_m^2 - \bar{\Omega}^2)} \exp(iT_0(-\bar{\omega}_m + \bar{\omega}_s + \bar{\Omega})) \\ & \frac{A_m^2 (\hat{F}_s - (e_0a)^2 \hat{G}_s)}{2(\bar{\omega}_s^2 - \bar{\Omega}^2)} \exp(iT_0(2\bar{\omega}_s + \bar{\Omega})) \\ & + \frac{(\hat{F}_s - (e_0a)^2 \hat{G}_s)(\hat{F}_m - (e_0a)^2 \hat{G}_m)^2}{8(\bar{\omega}_m^2 - \bar{\Omega}^2)(\bar{\omega}_s^2 - \bar{\Omega}^2)} \exp(iT_0(3\bar{\Omega})) \\ & \frac{A_m (\hat{F}_s - (e_0a)^2 \hat{G}_s)(\hat{F}_m - (e_0a)^2 \hat{G}_m)}{2(\bar{\omega}_m^2 - \bar{\Omega}^2)(\bar{\omega}_s^2 - \bar{\Omega}^2)} \exp(iT_0(2\bar{\Omega} + \bar{\omega}_m)) \\ & + \frac{A_m \bar{A}_m (\hat{F}_s - (e_0a)^2 \hat{G}_s)}{(\bar{\omega}_s^2 - \bar{\Omega}^2)} \exp(iT_0(\bar{\Omega})) \\ & \frac{3(\hat{F}_s - (e_0a)^2 \hat{G}_s)(\hat{F}_m - (e_0a)^2 \hat{G}_m)^2}{8(\bar{\omega}_m^2 - \bar{\Omega}^2)^2(\bar{\omega}_s^2 - \bar{\Omega}^2)} \exp(iT_0(\bar{\Omega})) \\ & + \frac{A_m (\hat{F}_s - (e_0a)^2 \hat{G}_s)(\hat{F}_m - (e_0a)^2 \hat{G}_m)}{(\bar{\omega}_m^2 - \bar{\Omega}^2)(\bar{\omega}_s^2 - \bar{\Omega}^2)} \exp(iT_0(\bar{\omega}_m)) \\ & + \frac{\bar{A}_m^2 (\hat{F}_s - (e_0a)^2 \hat{G}_s)}{2(\bar{\omega}_s^2 - \bar{\Omega}^2)} \exp(iT_0(-2\bar{\omega}_m + \bar{\Omega})) \\ & + \frac{\bar{A}_m (\hat{F}_s - (e_0a)^2 \hat{G}_s)(\hat{F}_m - (e_0a)^2 \hat{G}_m)}{2(\bar{\omega}_m^2 - \bar{\Omega}^2)(\bar{\omega}_s^2 - \bar{\Omega}^2)} \\ & \times \exp(iT_0(2\bar{\Omega} - \bar{\omega}_m)) + CC \quad (15) \end{aligned}$$

As seen, if $3\bar{\Omega} \approx \bar{\omega}_n$, the secondary resonance will occur.

To investigate the nonlinear forced vibration of nano-beams with secondary resonance, one should introduce a detuning parameter σ according to

$$3\bar{\Omega} = \bar{\omega}_n + \varepsilon^2 \sigma \tag{16}$$

After substituting Eq. (16) into Eq. (14), the secular terms will be eliminated from q_{n3} if:

$$\begin{aligned} & -a_n \sum_1^N m^2 \left(2A_n A_m \bar{A}_m + \frac{2(\hat{F}_m - (e_0 a)^2 \hat{G}_m)^2}{(\bar{\omega}_m^2 - \bar{\Omega}^2)^2} A_n \right. \\ & \left. + \frac{(\hat{F}_n - (e_0 a)^2 \hat{G}_n)(\hat{F}_m - (e_0 a)^2 \hat{G}_m)^2}{8(\bar{\omega}_m^2 - \bar{\Omega}^2)^2 (\bar{\omega}_n^2 - \bar{\Omega}^2)} \exp(i\sigma T_2) \right) \\ & - a_n \left[\frac{n^2 (\hat{F}_n - (e_0 a)^2 \hat{G}_n)^2}{2(\bar{\omega}_n^2 - \bar{\Omega}^2)^2} + n^2 \bar{A}_n A_n \right] A_n \\ & - 2i\bar{\omega}_n \frac{dA_n}{dT_2} - 2i\bar{\omega}_n \hat{C}_n A_n = 0 \end{aligned} \tag{17}$$

and the secular terms will be eliminated from q_{j3} (where $j = 1, \dots, M$ and $j \neq n$) if:

$$\begin{aligned} & -a_j \sum_1^N m^2 \left(2A_j A_m \bar{A}_m + \frac{2(\hat{F}_m - (e_0 a)^2 \hat{G}_m)^2}{(\bar{\omega}_m^2 - \bar{\Omega}^2)^2} A_j \right) \\ & - a_n \left[\frac{j^2 (\hat{F}_j - (e_0 a)^2 \hat{G}_j)^2}{2(\bar{\omega}_j^2 - \bar{\Omega}^2)^2} + j^2 \bar{A}_j A_j \right] A_j \\ & - 2i\bar{\omega}_j \frac{dA_j}{dT_2} - 2i\bar{\omega}_j \hat{C}_j A_j = 0 \end{aligned} \tag{18}$$

Substituting polar transformation ($A_s = \frac{1}{2} b_s \exp(i\theta_s)$, $s = j, m, n$) for A_m , A_n and A_j in Eqs. (17) and (18), and separating real and imaginary parts, one can obtain the following equations after some simplifications:

$$\begin{aligned} \bar{\omega}_j \theta'_j b_j = a_j \sum_{m=1}^N \frac{1}{4} m^2 \left(b_m^2 b_j + \frac{b_j (\hat{F}_m - (e_0 a)^2 \hat{G}_m)^2}{(\bar{\omega}_m^2 - \bar{\Omega}^2)^2} \right) \\ + \frac{a_j b_j}{2} \left[\frac{j^2 (\hat{F}_j - (e_0 a)^2 \hat{G}_j)^2}{(\bar{\omega}_j^2 - \bar{\Omega}^2)^2} + \frac{j^2 b_j^2}{4} \right] \end{aligned} \tag{19a}$$

$$\bar{\omega}_j b'_j = -\hat{C}_j b_j \bar{\omega}_j \tag{19b}$$

$$\begin{aligned} \gamma' = \frac{a_n}{b_n \bar{\omega}_n} \sum_{m=1}^N \frac{1}{4} m^2 \left(b_m^2 b_n + \frac{b_n (\hat{F}_m - (e_0 a)^2 \hat{G}_m)^2}{(\bar{\omega}_m^2 - \bar{\Omega}^2)^2} \right) \\ + \frac{a_n}{2\bar{\omega}_n} \left[\frac{n^2 (\hat{F}_n - (e_0 a)^2 \hat{G}_n)^2}{(\bar{\omega}_n^2 - \bar{\Omega}^2)^2} + \frac{n^2 b_n^2}{4} \right] + \frac{a_n}{b_n \bar{\omega}_n} \\ \times \sum_{m=1}^N m^2 \frac{(\hat{F}_n - (e_0 a)^2 \hat{G}_n)(\hat{F}_m - (e_0 a)^2 \hat{G}_m)^2}{8(\bar{\omega}_m^2 - \bar{\Omega}^2)^2 (\bar{\omega}_n^2 - \bar{\Omega}^2)} \cos(\gamma) - \sigma \end{aligned} \tag{19c}$$

$$\begin{aligned} \bar{\omega}_n b'_n = -\hat{C}_n b_n \bar{\omega}_n \\ + a_n \sum_{m=1}^N m^2 \frac{(\hat{F}_n - (e_0 a)^2 \hat{G}_n)(\hat{F}_m - (e_0 a)^2 \hat{G}_m)^2}{8(\bar{\omega}_m^2 - \bar{\Omega}^2)^2 (\bar{\omega}_n^2 - \bar{\Omega}^2)} \sin(\gamma) \end{aligned} \tag{19d}$$

where $(\cdot)' = \frac{d(\cdot)}{dT_2}$, $\gamma = (\theta_n - \sigma T_2)$, $j = 1, \dots, N$, and $j \neq n$.

Numerical integrating of Eqs. (19a)–(19d) and using Eqs. (6) and (10), one can obtain the lateral displacement of FG nano-beams under super-harmonic excitation as follows:

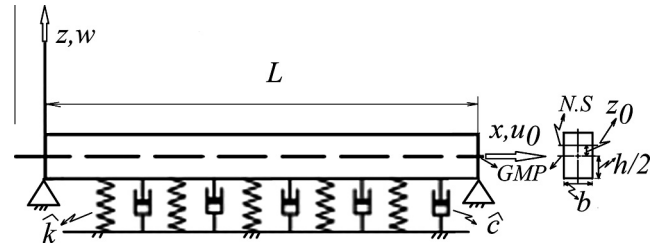


Figure 1 Schematic Geometry, coordinate system and boundary conditions of FG nano-beam resting on viscous foundation. GMP and N.S. stand for geometric mid-plane and neutral surface respectively.

$$\begin{aligned} \bar{W} = \sum_{s=1}^N \left(\varepsilon b_s \cos(\bar{\omega}_s \bar{t} + \theta_s) + \varepsilon \frac{(\hat{F}_s - (e_0 a)^2 \hat{G}_s)}{(\bar{\omega}_s^2 - \bar{\Omega}^2)} \cos(\bar{\Omega} \bar{t}) \right) \sin(s\pi \bar{x}) \\ + O(\varepsilon^3) \end{aligned} \tag{20}$$

3.1. Steady state response

The solution of Eq. (19b) is as follows:

$$b_j = \alpha_j \exp(-\hat{C}_j \varepsilon^2 t) \tag{21}$$

As seen, b_j ($j = 1, \dots, N$ and $j \neq n$) exponentially tends to zero. Consequently, the value of b_j ($j = 1, \dots, N$ and $j \neq n$) will be zero in Eqs. (19c) and (19d) when time tends to infinity. The values of b'_n and γ' must be equal to zero to study the steady-state response of excited FG nano-beams as well. Thus, the following relationship is obtained:

$$\begin{aligned} 0 = \frac{a_n}{b_n \bar{\omega}_n} \left(\frac{n^2 b_n^3}{4} + \sum_{m=1}^N \frac{m^2 b_n (\hat{F}_m - (e_0 a)^2 \hat{G}_m)^2}{4 (\bar{\omega}_m^2 - \bar{\Omega}^2)^2} \right) \\ + \frac{a_n}{2\bar{\omega}_n} \left[\frac{n^2 (\hat{F}_n - (e_0 a)^2 \hat{G}_n)^2}{(\bar{\omega}_n^2 - \bar{\Omega}^2)^2} + \frac{n^2 b_n^2}{4} \right] + \frac{a_n}{b_n \bar{\omega}_n} \\ \times \sum_{m=1}^N m^2 \frac{(\hat{F}_n - (e_0 a)^2 \hat{G}_n)(\hat{F}_m - (e_0 a)^2 \hat{G}_m)^2}{8(\bar{\omega}_m^2 - \bar{\Omega}^2)^2 (\bar{\omega}_n^2 - \bar{\Omega}^2)} \cos(\gamma) - \sigma \end{aligned} \tag{22}$$

$$0 = -\hat{C}_n b_n + \frac{a_n}{\bar{\omega}_n} \sum_{m=1}^N m^2 \frac{(\hat{F}_n - (e_0 a)^2 \hat{G}_n)(\hat{F}_m - (e_0 a)^2 \hat{G}_m)^2}{8(\bar{\omega}_m^2 - \bar{\Omega}^2)^2 (\bar{\omega}_n^2 - \bar{\Omega}^2)} \sin(\gamma) \tag{23}$$

The frequency-response equation can be found by eliminating γ from Eqs. (22) and (23) as follows:

$$\sigma = \pm \left[\frac{a_n^2 S_1^2}{b_n^2 \bar{\omega}_n^2} - \hat{C}_n^2 \right]^{1/2} + \frac{3b_n^2 n^2 a_n}{8\bar{\omega}_n} + \frac{1}{\bar{\omega}_n} \left[a_n S_2 + \frac{n^2 a_n (\hat{F}_n - (e_0 a)^2 \hat{G}_n)^2}{2(\bar{\omega}_n^2 - \bar{\Omega}^2)^2} \right] \tag{24}$$

where

$$S_2 = \sum_{m=1}^N \left(\frac{m^2 (\hat{F}_m - (e_0 a)^2 \hat{G}_m)^2}{4 (\bar{\omega}_m^2 - \bar{\Omega}^2)^2} \right) \tag{25}$$

$$S_1 = \sum_{m=1}^N m^2 \frac{(\hat{F}_n - (e_0 a)^2 \hat{G}_n)(\hat{F}_m - (e_0 a)^2 \hat{G}_m)^2}{8(\bar{\omega}_m^2 - \bar{\Omega}^2)(\bar{\omega}_n^2 - \bar{\Omega}^2)}$$

$$= \frac{(\hat{F}_n - (e_0 a)^2 \hat{G}_n)}{2(\bar{\omega}_n^2 - \bar{\Omega}^2)} S_2 \quad (26)$$

Based upon Eq. (24), the dimensionless peak response ($b_{n_{\max}}$) and the corresponding detuning (σ_{\max}) can be derived as follows:

$$b_{n_{\max}} = \frac{a_n S_1}{\hat{C}_n \bar{\omega}_n} \quad (27)$$

$$\sigma_{\max} = \frac{3b_n^2 n^2 a_n}{8\bar{\omega}_n} + \frac{1}{\bar{\omega}_n} \left[a_n S_2 + \frac{n^2 a_n (\hat{F}_n - (e_0 a)^2 \hat{G}_n)^2}{2(\bar{\omega}_n^2 - \bar{\Omega}^2)^2} \right] \quad (28)$$

According to Eq. (20), the steady-state deflection of excited FG nano-beam (\bar{W}_s) can be approximated as follows:

$$\bar{W}_s = \varepsilon b_n \cos((\bar{\omega}_n + \sigma \varepsilon^2) \bar{t} + \gamma) \sin(n\pi \bar{x})$$

$$+ \varepsilon \sum_{s=1}^M \left(\frac{(\hat{F}_s - (e_0 a)^2 \hat{G}_s)}{(\bar{\omega}_s^2 - \bar{\Omega}^2)} \cos(\bar{\Omega} \bar{t}) \sin(s\pi \bar{x}) \right) + O(\varepsilon^3) \quad (29)$$

where γ can be found by solving Eq. (23). As seen, the steady-state response of FG nano-beam to super-harmonic excitations is formed from the particular and free-oscillation solutions.

If the value of small scale parameter ($e_0 a$), the index of power-law (\bar{n}) and the coefficient of the stiffness of the foundation (\hat{k}) in all equations were set to zero and also if it was assumed that $3\bar{\Omega} = \bar{\omega}_1 + \varepsilon^2 \sigma$, Eq. (24) would be converted into the following equation which was in concordance with the equation proposed by Nayfeh and Mook [22]:

$$\sigma = + \frac{3b_1^2 \pi^2}{32} + \frac{\pi^2}{4} \left[\sum_{m=2}^N \frac{m^2 (\hat{F}_m)^2}{4((m\pi)^2 - \bar{\Omega}^2)^2} + \frac{3(\hat{F}_1)^2}{4(\pi^2 - \bar{\Omega}^2)^2} \right]$$

$$\pm \left[\frac{\pi^4 \left(\sum_{m=1}^N m^2 \frac{(\hat{F}_1)(\hat{F}_m)^2}{8((m\pi)^2 - \bar{\Omega}^2)^2 (\pi^2 - \bar{\Omega}^2)} \right)^2}{16b_1^2} - \hat{C}_n^2 \right]^{1/2} \quad (30)$$

It is worth mentioning that the linear mode shapes and the external force used by Nayfeh and Mook [22] are $\sqrt{2} \sin(s\pi \bar{x})$ and $2\hat{F}_s$ respectively which are different from those employed in the present study ($\sin(s\pi \bar{x})$ and \hat{F}_s). These differences between coefficients of the linear mode shapes and external force justify the difference between Eq. (30) and that obtained by Nayfeh and Mook [22].

4. Numerical results and discussion

Mechanical properties of silicon nitride (Si_3N_4) and stainless steel-grade 304 (SUS304) are used in the numerical analysis. It is assumed that the nano-beam is made of pure metal (stainless steel-grade 304) when the power-law index (\bar{n}) is zero and with a rise in the power-law index (\bar{n}), the volume fraction of silicon nitride gradually increases in nano-beam. Consequently, an increase in power-law index increases extensional and flexural stiffness of FG nano-beam. It is also assumed that operating frequency is nearly one-third of the lowest natural frequency.

According to Eq. (8), it is expected that a rise in nonlocal parameter and/or power-law index decreases the dimensionless natural frequencies. Eqs. (9a) and (9b) clearly reveal that the nonlocal parameter does not affect the dimensionless nonlinear term (a_s) and the dimensionless damping coefficient (\hat{C}_1).

The effects of an increase in index of power-law on dimensionless damping coefficient (\hat{C}_1) and the coefficient of nonlinear term are listed in Table 1. On the basis of Table 1, as long as the value of power-law index is lower than 0.06, the dimensionless coefficient of damping will decrease if the index of power-law increases. A rise in the power-law index which is more than 0.06 increases the dimensionless coefficient of damping. The coefficient of nonlinear term in Eq. (7) will continually increase if the index of power-law rises due to increasing the extensional-to-flexural stiffness ratio. The numerical results listed in Table 1 clearly show that the rate of the growth of the coefficient of nonlinear term is much more than that of the dimensionless coefficient of damping. Therefore, it is expected that with an increase in the index of power-law, the dimensionless value of peak response (Eq. (27)) and the corresponding detuning parameter (Eq. (28)) rise.

It is worth mentioning that the upper limit value of Eq. (25) affects the accurate prediction of the dimensionless peak response and the corresponding detuning parameter (it must be noted that one can rewrite S_1 on the basis of S_2 (see Eq. (26))). Tables 2, 3 and 4 clearly show the influence of small scale value, power law index, the kind of distributed lateral load and the upper limit value of Eq. (25) on the value of S_2 . According to these tables, the value of S_2 converges to a fixed value as increasing the upper limit value of Eq. (25). Then, the first ten sentences ($N = 10$) of Eq. (25) are used to estimate the dimensionless peak response and corresponding detuning parameter because more sentences rise the values of S_2 (Eq. (25)) less than 1×10^{-4} (see Tables 2-4) which can be negligible.

Backbone curves resulting from distributed lateral load with constant intensity are shown in Fig. 2 to investigate the effects of the small scale parameter and the index of power-law on the dimensionless peak response. As explained above, at a fixed value of nonlocal parameter, dimensionless peak response and corresponding detuning parameter increase with an increase in power-law index. It is also seen that, at a fixed value of power-law index, a rise in the nonlocal parameter decreases the dimensionless peak response and the corresponding detuning parameter due to the decrease in the dimensionless natural frequencies and the dimensionless lateral force as increasing small scale.

Based upon Eq. (9c), the type of distributed lateral load can affect the peak response and frequency-response curves. Three different kinds of distributed lateral load whose resultant forces are equal are used to study the effects of distributed lateral load with different intensities on frequency-response curves (Table 5). Fig. 3 demonstrates that the kind of distributed lateral load affects not only the value of the dimensionless peak response and the corresponding detuning but also the occurrence of the jumping phenomenon.

Figs. 2, 4 and 5 show how the type of distributed lateral load affects the influence of small scale parameter on dimensionless peak response.

As seen, with an increase in the index of power-law, the dimensionless peak response and the corresponding detuning

Table 1 The effect of an increase in index of power-law on dimensionless damping coefficient (\widehat{C}_1) and the coefficient of nonlinear term ($L/h = 25$ nm).

n		0	0.02	0.04	0.06	0.08	0.1	0.5	1	1.5
$h = 0.5$	\widehat{C}_1	10.79	10.76	10.73	10.68	10.67	10.77	11.11	11.42	11.67
	a_1	24.35	24.73	25.12	25.96	26.39	36.16	49.29	62.66	76.06
$h = 1$	\widehat{C}_1	2.699	2.690	2.682	2.672	2.668	2.693	2.778	2.855	2.917
	a_1	24.352	24.730	25.126	25.960	26.395	36.163	49.295	62.669	76.066
$h = 1.5$	\widehat{C}_1	1.199	1.195	1.192	1.187	1.186	1.196	1.234	1.269	1.296
	a_1	24.352	24.730	25.126	25.960	26.395	36.163	49.295	62.669	76.066
$h = 2$	\widehat{C}_1	0.6748	0.6725	0.6707	0.6680	0.6671	0.6732	0.6946	0.7139	0.7294
	a_1	24.352	24.730	25.126	25.960	26.395	36.163	49.295	62.669	76.066

Table 2 The effects of upper limit (N) of Eq. (25) on the values of S_2 for lateral distributed load with constant intensity. $S_2(N)$ means the value of S_2 on the basis of the first N sentences of Eq. (25).

e_0a	$S_2(10)-S_2(5)$				$S_2(15)-S_2(10)$			
	0	0.5	1	1.5	0	0.5	1	1.5
$\bar{n} = 0$	0.5×10^{-3}	0.5×10^{-3}	0.5×10^{-3}	0.5×10^{-3}	0.17×10^{-4}	0.17×10^{-4}	0.17×10^{-4}	0.17×10^{-4}
$\bar{n} = 0.03$	0.5×10^{-3}	0.5×10^{-3}	0.5×10^{-3}	0.4×10^{-3}	0.16×10^{-4}	0.16×10^{-4}	0.16×10^{-4}	0.16×10^{-4}
$\bar{n} = 0.06$	0.4×10^{-3}	0.4×10^{-3}	0.4×10^{-3}	0.4×10^{-3}	0.15×10^{-4}	0.15×10^{-4}	0.15×10^{-4}	0.15×10^{-4}
$\bar{n} = 0.09$	0.4×10^{-3}	0.4×10^{-3}	0.4×10^{-3}	0.4×10^{-3}	0.15×10^{-4}	0.15×10^{-4}	0.15×10^{-4}	0.14×10^{-4}
$\bar{n} = 0.12$	0.4×10^{-3}	0.4×10^{-3}	0.4×10^{-3}	0.4×10^{-3}	0.14×10^{-4}	0.14×10^{-4}	0.14×10^{-4}	0.14×10^{-4}

Table 3 The effects of upper limit (N) of Eq. (25) on the values of S_2 for lateral distributed load shown by L2 in Table 5. $S_2(N)$ means the value of S_2 on the basis of the first N sentences of Eq. (25).

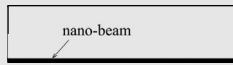
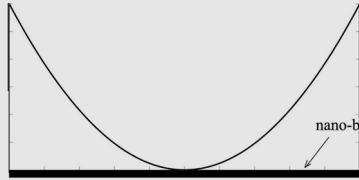
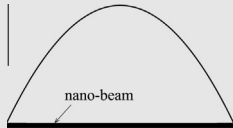
e_0a	$S_2(10)-S_2(5)$				$S_2(15)-S_2(10)$			
	0	0.5	1	1.5	0	0.5	1	1.5
$\bar{n} = 0$	4.7×10^{-3}	4.6×10^{-3}	4.5×10^{-3}	4.3×10^{-3}	0.15×10^{-3}	0.15×10^{-3}	0.15×10^{-3}	0.14×10^{-3}
$\bar{n} = 0.03$	4.4×10^{-3}	4.4×10^{-3}	4.2×10^{-3}	4.0×10^{-3}	0.14×10^{-3}	0.14×10^{-3}	0.14×10^{-3}	0.13×10^{-3}
$\bar{n} = 0.06$	4.2×10^{-3}	4.2×10^{-3}	4×10^{-3}	3.8×10^{-3}	0.14×10^{-3}	0.13×10^{-3}	0.13×10^{-3}	0.13×10^{-3}
$\bar{n} = 0.09$	4.0×10^{-3}	4.0×10^{-3}	3.9×10^{-3}	3.7×10^{-3}	0.13×10^{-3}	0.13×10^{-3}	0.13×10^{-3}	0.12×10^{-3}
$\bar{n} = 0.12$	3.9×10^{-3}	3.8×10^{-3}	3.7×10^{-3}	3.5×10^{-3}	0.12×10^{-3}	0.12×10^{-3}	0.12×10^{-3}	0.12×10^{-3}

Table 4 The effects of upper limit (N) of Eq. (25) on the values of S_2 for lateral distributed load shown by L3 in Table 5. $S_2(N)$ means the value of S_2 on the basis of the first N sentences of Eq. (25).

e_0a	$S_2(10)-S_2(5)$				$S_2(15)-S_2(10)$			
	0	0.5	1	1.5	0	0.5	1	1.5
$\bar{n} = 0$	0.3×10^{-6}	0.4×10^{-6}	0.9×10^{-6}	2×10^{-6}	0.1×10^{-8}	0.3×10^{-8}	1×10^{-8}	4×10^{-8}
$\bar{n} = 0.03$	0.2×10^{-6}	0.4×10^{-6}	0.9×10^{-6}	2×10^{-6}	0.1×10^{-8}	0.3×10^{-8}	1×10^{-8}	4×10^{-8}
$\bar{n} = 0.06$	0.2×10^{-6}	0.3×10^{-6}	0.8×10^{-6}	2×10^{-6}	0.1×10^{-8}	0.3×10^{-8}	1×10^{-8}	4×10^{-8}
$\bar{n} = 0.09$	0.2×10^{-6}	0.3×10^{-6}	0.8×10^{-6}	2×10^{-6}	0.1×10^{-8}	0.29×10^{-8}	1×10^{-8}	4×10^{-8}
$\bar{n} = 0.12$	0.2×10^{-6}	0.3×10^{-6}	0.8×10^{-6}	1.9×10^{-6}	0.1×10^{-8}	0.28×10^{-8}	1×10^{-8}	3.9×10^{-8}

parameter rise regardless of changing the distributed lateral load while the effects of the small scale parameter on the peak response completely depend on the kind of the distributed load.

The influence of stiffness and damping coefficient of foundation on frequency-response curves is studied as well. According to Eq. (8), it is expected that an increase in stiffness of foundation increases the dimensionless natural frequencies

Symbol	Formula	Sketch
C	$F = nF(\frac{1}{3}) \cos(\bar{\Omega}t)$	
L2	$F = nF(4x^2 - 4x + 1) \cos(\bar{\Omega}t)$	
L3	$F = nF(-2x^2 + 2x) \cos(\bar{\Omega}t)$	

nF is a scale factor.

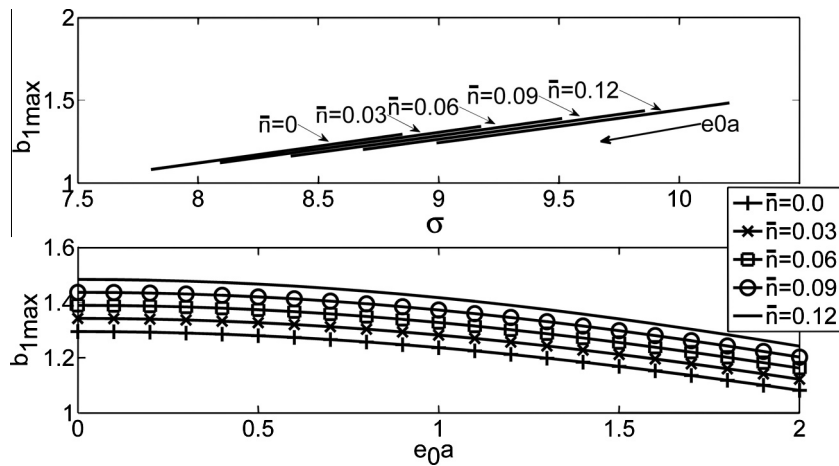


Figure 2 The effects of small scale parameter and index of power-law on peak response and corresponding detuning resulting from distributed lateral load with constant intensity (DimC = 2.67, DimK = 2.33e3 when $\bar{n} = 0$).

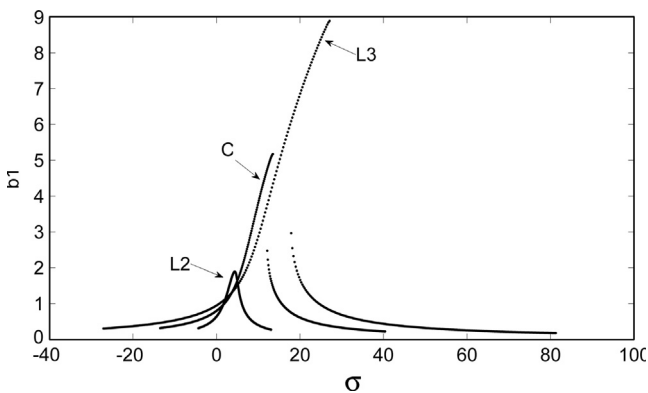


Figure 3 The effects of the type of distributed lateral load on frequency-response curves of excited FG nano-beams (DimC = 2.67, DimK = 2.33e3, $\bar{n} = 0$, $e_0a = 0$).

appearing in denominator of Eq. (27). Thus, with an increase in the stiffness of foundation, the dimensionless peak response decreases. Fig. 6 clearly shows the effects of stiffness of foundation on frequency-response curves of FG nano-beams under distributed lateral load with constant intensity. As seen, with a decrease in stiffness of foundation not only the dimensionless peak response and the corresponding detuning increase but also the amplitude curve bends more. In Fig. 6, 'DimK' which equals $\hat{k}L^4/D$ stands for the dimensionless stiffness of foundation.

Fig. 7 that shows the effects of damping on the frequency-response curves clearly reveals that with an increase in damping coefficient, the dimensionless peak response increases and frequency-response curves bend more to the right-hand side. This behavior is expected because of the appearance of damping coefficient in denominator of Eq. (27). In Fig. 7, 'DimC' that equals $\hat{c}L^2/\sqrt{D\rho_e}$ stands for the dimensionless damping coefficient of foundation. The distributed lateral load with constant intensity is used to plot Fig. 7.

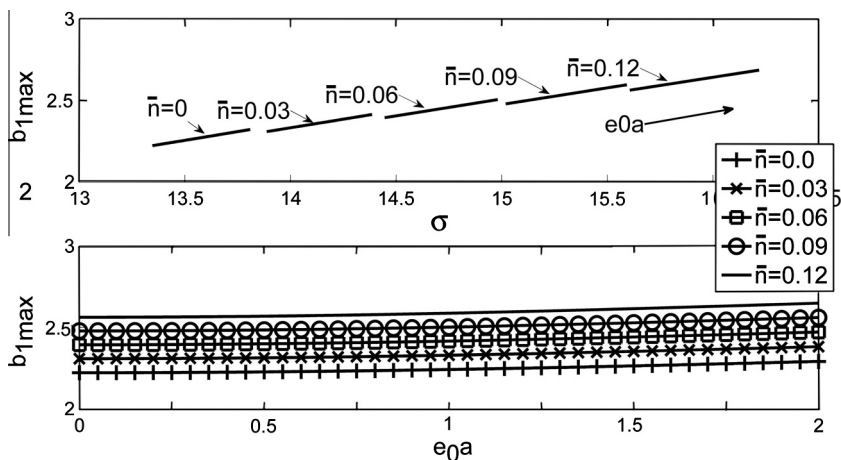


Figure 4 The effects of small scale parameter and index of power-law on peak response and corresponding detuning resulting from distributed lateral load presented with L3 in Table 5 (DimC = 2.67, DimK = 2.33e3 when $\bar{n} = 0$).

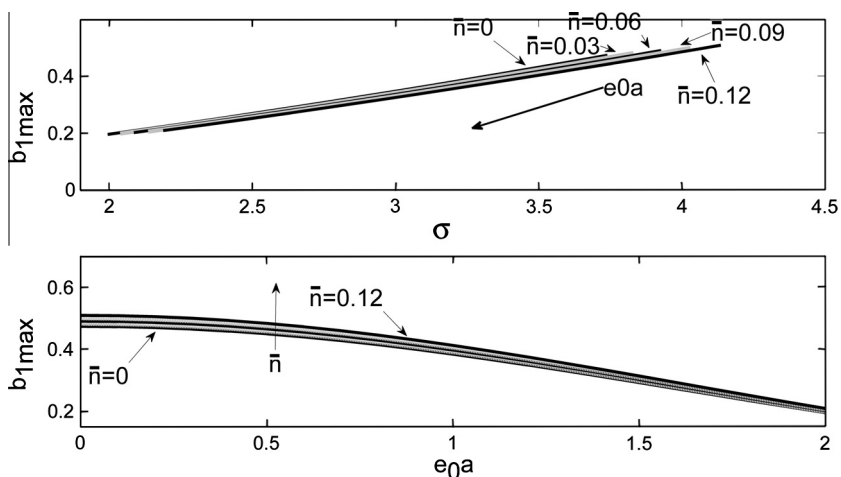


Figure 5 The effects of small scale parameter and index of power-law on peak response and corresponding detuning resulting from distributed lateral load presented with L2 in Table 5 (DimC = 2.67, DimK = 2.33e3 when $\bar{n} = 0$).

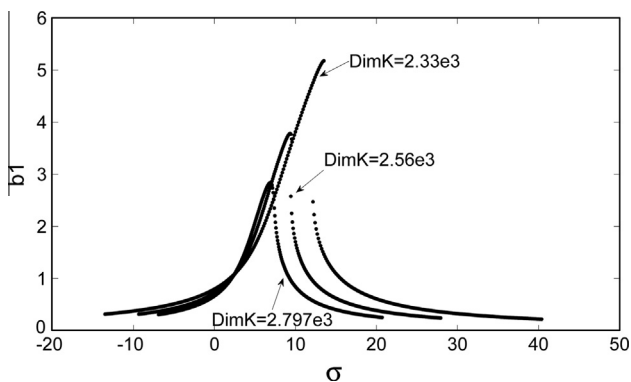


Figure 6 The influence of stiffness of foundation on frequency-response curves of excited FG nano-beams under distributed lateral load with constant intensity (DimC = 2.67, $\bar{n} = 0$, $e_0a = 0$).

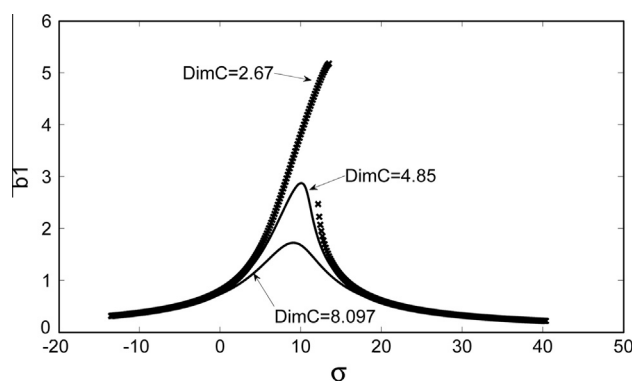


Figure 7 The influence of damping coefficient of foundation on frequency-response curves of FG nano-beams under distributed lateral load with constant intensity (DimK = 2.33e3, $\bar{n} = 0$, $e_0a = 0$).

5. Conclusion

This article is an attempt to study the effects of different parameters such as the stiffness and the damping coefficients of foundation, the index of power-law, the small scale parameter and the kind of distributed harmonic load on steady-state response of FG nano-beam under super-harmonic excitation. Multiple scale method is employed in order to derive the governing equations of steady state response of FG nano-beams excited by distributed harmonic force.

The results show that the effects of small scale parameter on backbone curves completely depend on the kind of loading. It is seen that with a decrease in the stiffness coefficient or with an increase in the damping coefficient, the dimensionless peak response increases and frequency-response curve bends more to the right-hand side as well.

Acknowledgment

The author gratefully acknowledges the support of Yasouj University under Grant No. Gryu-89111109.

Appendix A

The following equations are the equations of motion of a simply supported FG nano-beam with immovable ends derived by using Hamilton's principle. Based upon the previous research [16,18,20], it is also assumed that the in-plane inertia and the rotary inertia are negligible:

$$\frac{\partial \hat{N}}{\partial x} = 0 \quad (\text{A1})$$

$$F - \hat{k}W - \hat{c} \frac{\partial W}{\partial t} - \frac{\partial^2 \hat{M}}{\partial x^2} + \hat{N} \frac{\partial^2 W}{\partial x^2} = \left(\int_{A_0} \rho(z) dA_0 \right) \frac{\partial^2 W}{\partial t^2} \quad (\text{A2})$$

in which $W = W(x, t)$ is the transverse displacement of any point on the geometric mid-plane ($z = 0$, based on Fig. 1) of FG nano-beam element, $\rho(z)$ is the mass density which is functionally graded in the thickness direction, the axial normal force and the bending moment are shown by \hat{N} and \hat{M} respectively, \hat{k} and \hat{c} denote the stiffness of the foundation and the damping coefficient of the foundation respectively and $F = F(x) \cos(\Omega t)$ is a transverse loading.

According to Euler-Bernoulli hypothesis and von-Karman type geometrical nonlinearity, one can write the strain displacement relationship as follows [16,18,20]:

$$\varepsilon_x = \frac{\partial u_1}{\partial x} + \frac{1}{2} \left(\frac{\partial W}{\partial x} \right)^2 \quad (\text{A3})$$

in which u_1 denotes the total displacement along the x direction given by Eq. (A4).

$$u_1(x, z, t) = u_0(x, t) - (z - z_0) \frac{\partial W}{\partial x} \quad (\text{A4})$$

where $u_0(x, t)$ is an axial displacement of any point on the geometric mid-plane ($z = 0$, based on Fig. 1) of the FG nano-beam element. z_0 is the distance between the neutral surface and the geometric mid-plane of the FG nano-beam ($z = 0$, based on Fig. 1) [14]. According to the physical concept of the neutral surface, z_0 can be written as follows [14]:

$$z_0 = \frac{\int_{A_0} z E(z) dA_0}{\int_{A_0} E(z) dA_0} \quad (\text{A5})$$

Based on Eringen's nonlocal elasticity, stress-strain relationship is as follows:

$$\sigma_x - (e_0 a)^2 \nabla^2 \sigma_x = E \varepsilon_x \quad (\text{A6})$$

where $e_0 a$ is a material length scale parameter which contains material constant and internal characteristic length. On the other hand, resultant axial force and resultant moment (\hat{N} and \hat{M}) are as follows:

$$\hat{N} = \int_{A_0} \sigma_x dA_0, \quad \hat{M} = - \int_{A_0} \sigma_x (z - z_0) dA_0 \quad (\text{A7})$$

Substituting Eqs. (A3) and (A6) into (A7), one can obtain the stress resultants on a beam element:

$$\hat{N} - (e_0 a)^2 \nabla^2 \hat{N} = \left(\int_{A_0} E(z) dA_0 \right) \left[\frac{\partial u}{\partial x} + \frac{1}{2} \left(\frac{\partial W}{\partial x} \right)^2 \right] \quad (\text{A8a})$$

$$\hat{M} - (e_0 a)^2 \nabla^2 \hat{M} = \left(\int_{A_0} (z - z_0)^2 E(z) dA_0 \right) \frac{\partial^2 W}{\partial x^2} \quad (\text{A8b})$$

where $E(z)$ and $\rho(z)$ defined by Eq. (A9) are Young's modulus and specific mass density of FG beam material respectively.

$$E(z) = E_1 + (E_2 - E_1) \left(\frac{2z + h}{2h} \right)^{\bar{n}} \quad (\text{A9a})$$

$$\rho(z) = \rho_1 + (\rho_2 - \rho_1) \left(\frac{2z + h}{2h} \right)^{\bar{n}} \quad (\text{A9b})$$

in which E_i and ρ_i ($i = 1, 2$) are Young's modulus and specific mass density of the two materials used in construction of FG beam respectively.

The partial differential equation of transverse motion of FG nano-beams will be derived by combining Eqs. (A8b) and (A2) and making some simplifications:

$$\begin{aligned} (e_0 a)^2 H + \hat{N} \frac{\partial^2 W}{\partial x^2} - \hat{k}W - \hat{c} \frac{\partial W}{\partial t} + F(x, t) \\ = \left(\int_{A_0} (z - z_0)^2 E(z) dA_0 \right) \frac{\partial^4 W}{\partial x^4} + \left(\int_{A_0} \rho(z) dA_0 \right) \frac{\partial^2 W}{\partial t^2} \end{aligned} \quad (\text{A10})$$

where H is defined by Eq. (A11):

$$H = \hat{c} \frac{\partial^3 W}{\partial x^2 \partial t} + \hat{k} \frac{\partial^2 W}{\partial x^2} - \frac{\partial^2 F}{\partial x^2} - \hat{N} \frac{\partial^4 W}{\partial x^4} + \left(\int_{A_0} \rho(z) dA_0 \right) \frac{\partial^4 W}{\partial x^2 \partial t^2} \quad (\text{A11})$$

On the basis of Eq. (A1), one can conclude that $\nabla^2 \hat{N}$ is zero. Therefore, Eq. (A8a) is simplified as follows [16,18]:

$$\hat{N} = \left(\int_{A_0} E(z) dA_0 \right) \left[\frac{\partial u_0}{\partial x} + \frac{1}{2} \left(\frac{\partial W}{\partial x} \right)^2 \right] \quad (\text{A12a})$$

Integrating Eq. (A12a) yields [10,12,14]:

$$\int_0^L \hat{N} dx = \int_0^L \left(\left(\int_{A_0} E(z) dA_0 \right) \left[\frac{\partial u_0}{\partial x} + \frac{1}{2} \left(\frac{\partial W}{\partial x} \right)^2 \right] \right) dx \quad (\text{A13a})$$

or

$$\widehat{N}L = \left(\int_{A_0} E(z) dA_0 \right) \left[u_0(L) - u_0(0) + \int_0^L \frac{1}{2} \left(\frac{\partial W}{\partial x} \right)^2 dx \right] \quad (\text{A13b})$$

in which L denotes the length of beam. The boundary values of axial displacement of nano-beams are [16]:

$$u_0(0) = 0, \quad u_0(L) = 0 \quad (\text{A14})$$

Substituting for boundary conditions from Eq. (A14) into Eq. (A13b), one can obtain the relationship between axial force \widehat{N} and transverse displacement of mid-plane of nano-beams:

$$\widehat{N} = + \frac{1}{2L} \left(\int_{A_0} E(z) dA_0 \right) \int_0^L \left(\frac{\partial W}{\partial x} \right)^2 dx \quad (\text{A15})$$

Substituting for \widehat{N} from Eq. (A15) into Eqs. (A10) and (A11), one can acquire the governing equation of nonlinear forced lateral vibration of FG nano-beams.

References

- [1] A.S. Kanani, H. Niknam, A.R. Ohadi, M.M. Aghdam, Effect of nonlinear elastic foundation on large amplitude free and forced vibration of functionally graded beam, *Compos. Struct.* 115 (2014) 60–68.
- [2] M. Simsek, H.H. Yurtcu, Analytical solutions for bending and buckling of functionally graded nano-beams based on the nonlocal Timoshenko beam theory, *Compos. Struct.* 97 (2013) 378–386.
- [3] J.N. Reddy, Microstructure-dependent couple stress theories of functionally graded beams, *J. Mech. Phys. Solids* 59 (9) (2011) 2382–2399.
- [4] A. Arbind, J.N. Reddy, Nonlinear analysis of functionally graded microstructure-dependent beams, *Compos. Struct.* 98 (2013) 272–281.
- [5] M.A. Eltaher, A. Khairy, A.M. Sadoun, F.-A. Omar, Static and buckling analysis of functionally graded Timoshenko nanobeams, *Appl. Math. Comput.* 229 (2014) 283–295.
- [6] M.A. Eltaher, S.A. Emam, F.F. Mahmoud, Static and stability analysis of nonlocal functionally graded nanobeams, *Compos. Struct.* 96 (2013) 82–88.
- [7] M. Şimşek, H.H. Yurtcu, Analytical solutions for bending and buckling of functionally graded nanobeams based on the nonlocal Timoshenko beam theory, *Compos. Struct.* 97 (2013) 378–386.
- [8] P. Asgharifard Sharabiani, M.R. Haeri Yazdi, Nonlinear free vibrations of functionally graded nanobeams with surface effects, *Compos. Part B – Eng.* 45 (2013) 581–586.
- [9] Sh. Hosseini-Hashemi, R. Nazemnezhad, An analytical study on the nonlinear free vibration of functionally graded nanobeams incorporating surface effects, *Compos. Part B – Eng.* 52 (2013) 199–206.
- [10] R. Ansari, R. Gholami, S. Sahmani, Free vibration analysis of size-dependent functionally graded microbeams based on the strain gradient Timoshenko beam theory, *Compos. Struct.* 94 (2011) 221–228.
- [11] R. Ansari, R. Gholami, M. Faghih Shojaei, V. Mohammadi, S. Sahmani, Size-dependent bending, buckling and free vibration of functionally graded Timoshenko microbeams based on the most general strain gradient theory, *Compos. Struct.* 100 (2013) 385–397.
- [12] A.R. Setoodeh, S. Afrahim, Nonlinear dynamic analysis of FG micro-pipes conveying fluid based on strain gradient theory, *Compos. Struct.* 116 (2014) 128–135.
- [13] M.A. Eltaher, S.A. Emam, F.F. Mahmoud, Free vibration analysis functionally graded size-dependent nano-beams, *Appl. Math. Comput.* 218 (2012) 7406–7420.
- [14] M.A. Eltaher, A.E. Alshorbagy, F.F. Mahmoud, Determination of neutral axis position and its effect on natural frequencies of functionally graded macro/nano-beams, *Compos. Struct.* 99 (2013) 193–201.
- [15] B. Uymaz, Forced vibration analysis of functionally graded beams using nonlocal elasticity, *Compos. Struct.* 105 (2013) 227–239.
- [16] R. Nazemnezhad, Sh. Hosseini-Hashemi, Nonlocal nonlinear free vibration of functionally graded nano-beams, *Compos. Struct.* 110 (2014) 192–199.
- [17] O. Rahmani, O. Pedram, Analysis and modeling the size effect on vibration of functionally graded nano-beams based on nonlocal Timoshenko beam theory, *Int. J. Eng. Sci.* 77 (2014) 55–70.
- [18] H. Niknam, M.M. Aghdam, A semi analytical approach for large amplitude free vibration and buckling of nonlocal FG beams resting on elastic foundation, *Compos. Struct.* 119 (2015) 452–462.
- [19] K. Kiani, Longitudinal and transverse instability of moving nanoscale beam-like structures made of functionally graded materials, *Compos. Struct.* 107 (2014) 610–619.
- [20] S.A. Emam, A.H. Nayfeh, Postbuckling and free vibration of composite beams, *Compos. Struct.* 88 (2009) 636–642.
- [21] A.H. Nayfeh, S.A. Emam, Exact solution and stability of postbuckling configurations of beams, *Nonlinear Dyn.* 54 (2008) 395–408.
- [22] A.H. Nayfeh, D.T. Mook, *Nonlinear Oscillations*, John Wiley and Sons, Inc., 1995.